

## Supplementary File

**Supplementary Table S1.** List of NanoString gene probes included in the Pan Cancer Progression Panel and mapping to respective pathways

**Supplementary Table S2.** Primer Sequences (5'-3') for qRT-PCR validation

**Supplementary Table S3.** Genes incorporated in the FFPE DNA NGS Assay (n = 225)

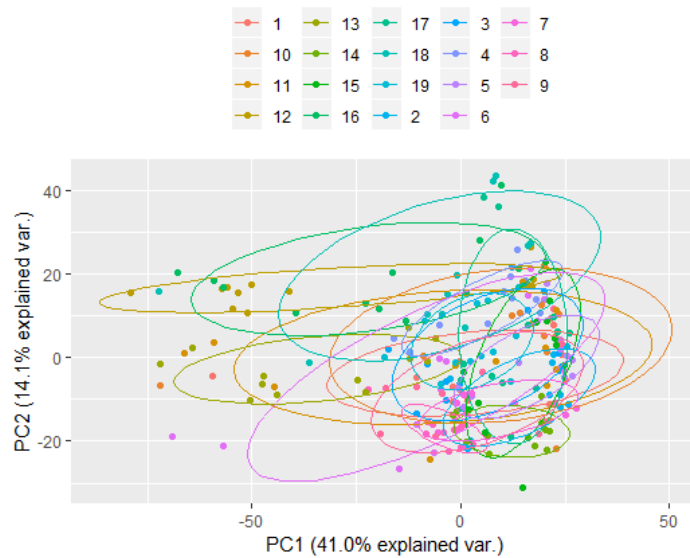
**Supplementary Table S4.** Sample list and various analyses performed per section

**Supplementary Table S5.** Clinical Characteristics of GC samples used in the study

**Supplementary Table S6.** NanoString results of GC ITH study

Matrix of 64 GC tumors with NanoString profiling of 770 genes per subregion for up to 4 subregions (PT<sub>sup1</sub>, PT<sub>sup2</sub>, PT<sub>deep</sub>, LN<sub>met</sub>). Results presented are in the normalized and log<sub>2</sub> transformed after quality control check flags were addressed. Of the 228 samples from 64 tumors that underwent Nanostring analysis, one sample failed internal QC checks as detected by nSolver. This sample's data was manually inspected, and was found to have a QC flag on Limit of Detection. In this sample, one positive control (out of 12 positive and negative controls) had a value lower than expected. According to the NanoString manual, a single control leading to the QC flag does not imply the failure of the sample and the results can generally be used. Manual inspection of the data on this sample did not reveal any other obviously abnormal readings, and hence this sample was not excluded from analysis.

Batch effects – as the Nanostring sampling was conducted in 19 batches (of 12 samples each), a PCA was conducted to analyse for batch effects. No obvious batch effect was detectable.



**Supplementary Table S7.** Volcano plot analysis of matched PT<sub>sup</sub> vs. PT<sub>deep</sub> analysis.

**Supplementary Table S8.** Volcano plot analysis of matched PT<sub>sup</sub> vs. LN<sub>met</sub> analysis.

**Supplementary Table S9.** Volcano plot analysis of matched PT<sub>deep</sub> vs. LN<sub>met</sub> analysis.

For tables S7, S8 and S9 data provided included – gene, p value of Wilcoxon two-sided paired (signed-rank) analysis, q value after correction for multiple hypothesis testing by FDR method, fold change (log<sub>2</sub>).

**Supplementary Table S10.** ITH grouping of samples.

Samples were classified as ITH<sub>high</sub> and ITH<sub>low</sub>. ITH was quantified by calculating the arithmetic mean of the standard deviations (SD) of gene expression between subregions per gene for each tumor. GC with mean SD > 50th centile were classified as ITH<sub>high</sub> while the rest as ITH<sub>low</sub>.

**Supplementary Table S11.** Comparison of clinical characteristics between ITH<sub>high</sub> and ITH<sub>low</sub> groups

**Supplementary Table S12.** Median SD of genes between subregions per GC.

**Supplementary Table S13.** Tumor/stroma ratio by subregion per GC

**Supplementary Table S14.** NGS DNA analysis of GC ITH by subregion.

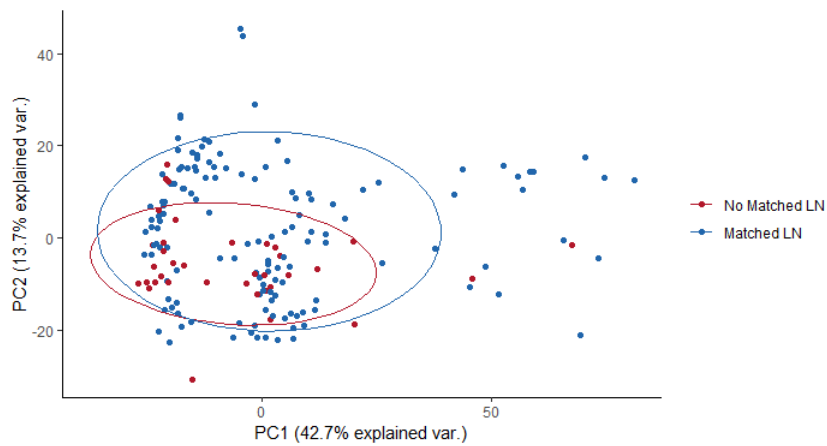
Only variants with moderate or high impact, called using VarDict, with maximum population variant frequency > 0.00001 and number of alternate supporting reads > 10 were considered for further analyses and depicted in the table.

**Supplementary Table S15.** Clinical characteristics of additional samples used in MLPA analysis (n = 20).

**Supplementary Table S16.** MLPA data of GC ITH study

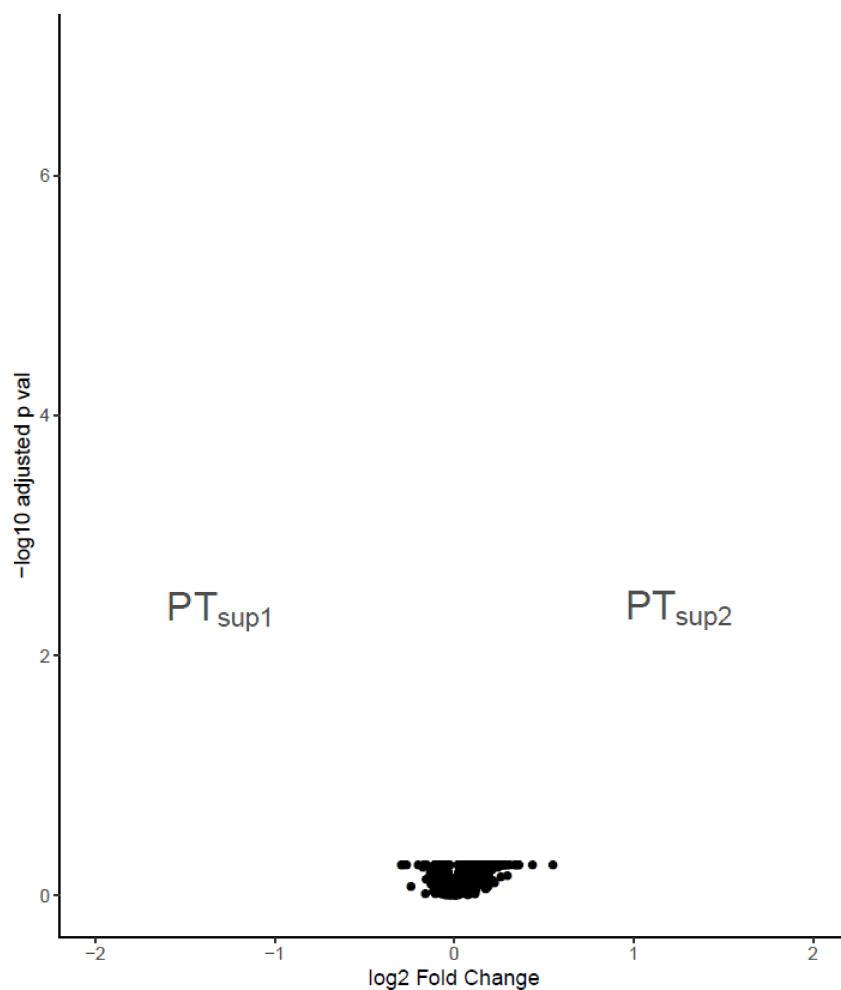
**Supplementary Table S17.** Phenotypic intra-tumoral spatial heterogeneity.

Samples were classified based on three main phenotypes: poorly cohesive -, non-poorly cohesive -, and mucinous phenotype. For poorly cohesive phenotype, the presence of signet-ring cells was divided into three categories: containing <10%, 10-90%, or ≥90% signet-ring cells

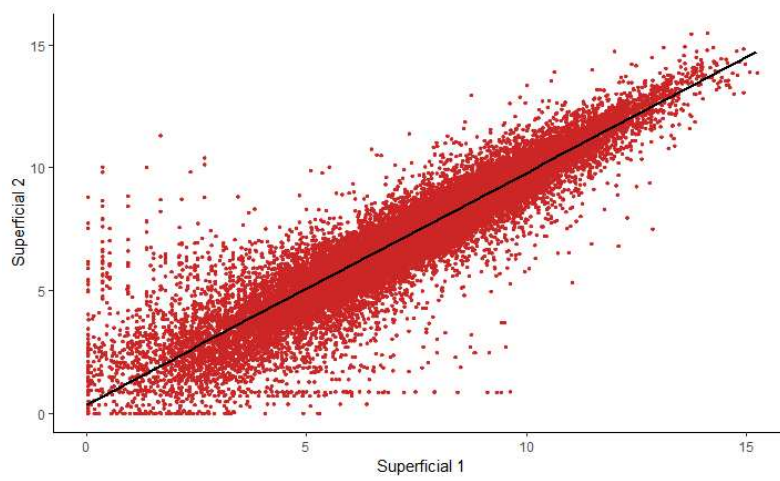


**Supplementary Figure S1.** Principal component analysis of NanoString data comparing primary tumors of GCs which had matched LN<sub>met</sub> and those that did not

Principal component analysis of NanoString data comparing primary tumor subregions of GCs which had matched LN<sub>met</sub> (n = 51), in blue, and those which did not (n = 13), in red. Complete overlap between the two groups suggest no systematic bias in the transcriptomic features for those samples with missing matched LN<sub>met</sub>.

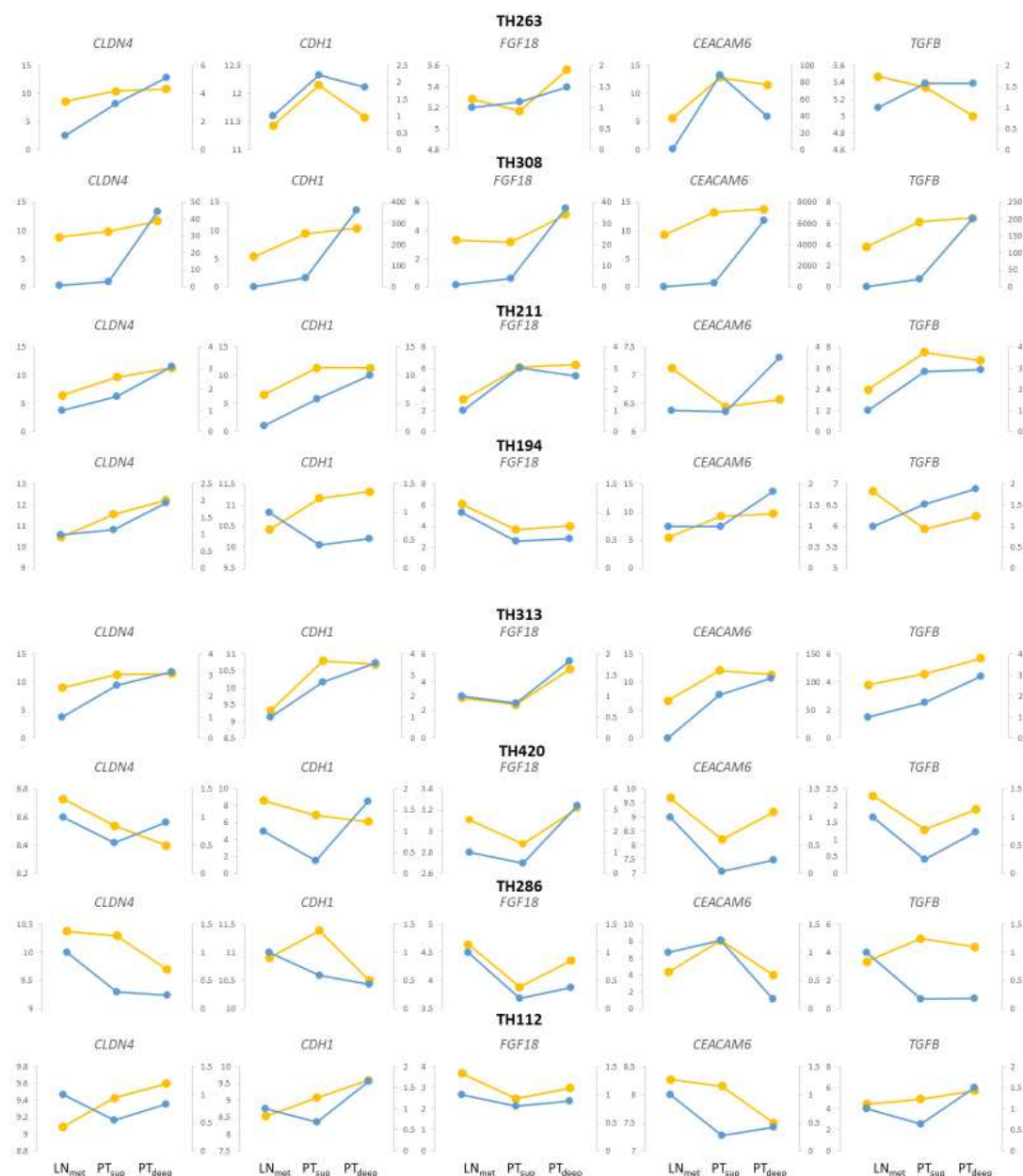


**Supplementary Figure S2.** Volcano plot of 770 genes from the Nanostring PanCancer Progression Panel compared between PT<sub>sup1</sub> and PT<sub>sup2</sub>. The x-axis is the log<sub>2</sub> fold change (log<sub>2</sub>FC) of gene expression between PT<sub>sup1</sub> and PT<sub>sup2</sub>. The y-axis is the -log<sub>10</sub> adjusted p-value results (FDR correction). There is no difference in expression between the two subregions, resulting in all plots clustering toward 0 on the x-axis and non-significant p-values.



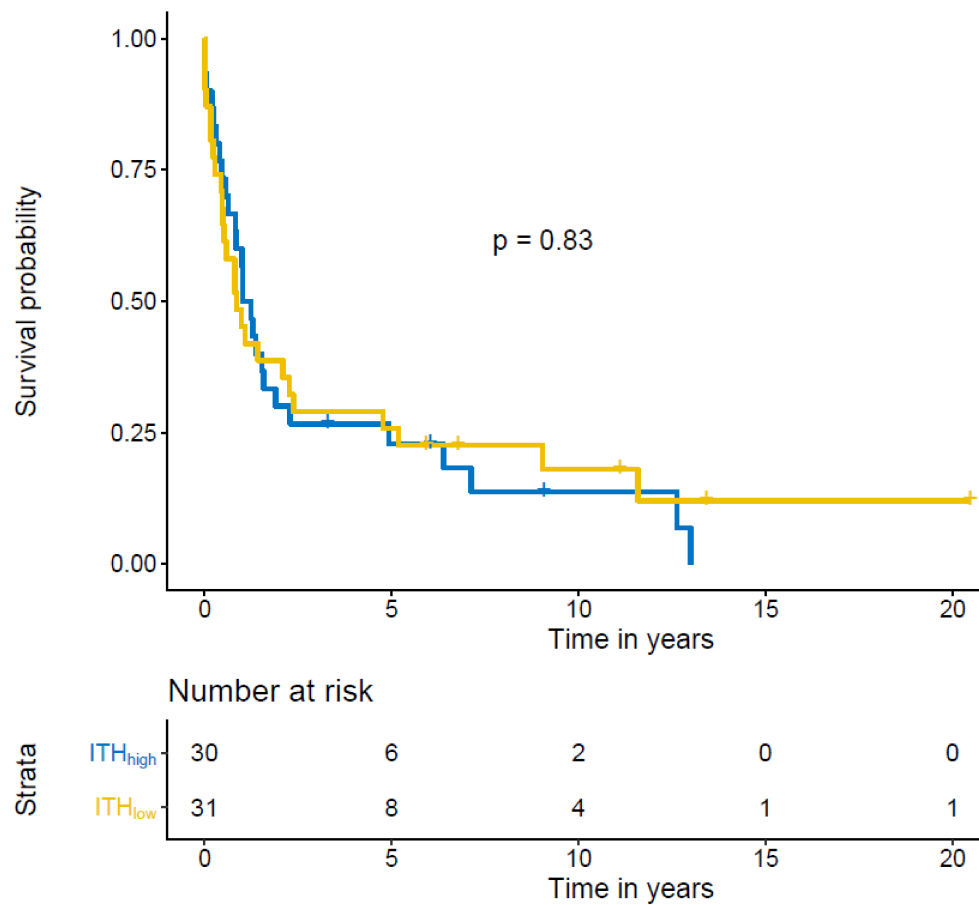
**Supplementary Figure S3.** Scatter plot correlating PT<sub>sup1</sub> and PT<sub>sup2</sub>

54 samples had paired PT<sub>sup1</sub> and PT<sub>sup2</sub> gene expression of 770 genes from NanoString. Spearman's  $R = 0.95$ ,  $p < 0.0001$



**Supplementary Figure S4.** qRT-PCR validation of NanoString results

qRT-PCR validation was performed in triplicate for 5 genes (*CLDN4*, *CDH1*, *FGF18*, *CEACAM6* and *TGFB2*) for 8 samples x 3 subregions, (PT<sub>sup</sub>, PT<sub>deep</sub>, LN<sub>met</sub>). Relative quantification values (RQ) of qRT-PCR results are depicted in blue dots with axes values on the left, while NanoString log<sub>2</sub> transformed gene expression is depicted in yellow dots with axes values on the right of each individual graph. In general, good correlation is seen between NanoString expression data and qRT-PCR results.



**Supplementary Figure S5.** Kaplan-Meier curve of overall survival in years of GC samples by ITH

GC were classified into ITH<sub>high</sub> (blue) and ITH<sub>low</sub> (yellow) based on the mean standard deviation of gene expression between subregions. There was no significant survival difference between the two groups.